

THE BORIDING PROCESS: GROWTH KINETICS AND MECHANICAL CHARACTERIZATION OF BORIDE LAYERS**I. Campos-Silva***

*Instituto Politécnico Nacional, Surface Engineering Group, SEPI-ESIME, U.P. Adolfo López Mateos, Zacatenco, México D.F., 07738, México,

Abstract:

Boriding is a thermochemical surface treatment in which boron diffuses into and combines with a substrate material to form a single- or double-phase metal boride layer at the substrate's surface. This contribution discusses the importance of boriding for ferrous materials in which the formation of boride layers, such as FeB and Fe₂B, improves hardness, wear resistance, temperature resistance and corrosion resistance at the surface of steels. The article includes a discussion of the growth kinetics of boride layers associated with a diffusion model. To understand the intended industrial applications, the article then reviews the mechanical characterisation by induced-fracture Vickers indentation and Berkovich nanoindentation of the boride layers.

Keywords: boriding; boride layers; growth kinetics; diffusion model; mechanical characterization; fracture resistance; Berkovich nanoindentation; hardness; thermal residual stress.

1. Introduction

Boriding, is a thermochemical surface treatment, whereby boron is diffused into, and combines with, the substrate material forming a single or double phase metal boride layer at the surface. Unlike many other surface treatments, hard boride layers can be developed on most alloys and metals by boron diffusion. The boriding of ferrous materials results in the formation of either a single layer (Fe₂B) or double-layer (FeB/Fe₂B) with definite composition. The phase equilibrium diagram of the binary system iron-boron shows the existence of two iron borides: Fe₂B with 9 wt. % B approximately, and FeB with 16.4 wt. % B approximately. The formation of either a single or double phase depends on the availability of boron. The formation of the Fe₂B layer is more desirable than a double-phase layer with FeB. The boron-rich FeB phase is considered undesirable because the FeB is more brittle than the Fe₂B. Therefore, the FeB phase should be avoided or minimized in the boride layer [1,2]. Borided parts have been used in a wide variety of industrial applications. The high hardness of borided materials makes them suited to resisting wear, particularly to that caused by abrasive particles. The wear resistance performances are obtained when contact stresses are minimized. The hardness of boride layers on iron materials is about 1800 to 2100 HV and higher for high-alloy steels.

The thickness of the layer formed (known as the case depth), which affects the mechanical and chemical behavior of borided steels, depends on the boriding temperature, the treatment time and the boron potential that surrounds the surface sample.

The optimum boride layer thickness for low-carbon steels and low-alloy steels ranges from 50 mm to 250 mm, while the optimum boride layer thickness for high-alloy steels ranges from 25 mm to 76 mm [2]. In addition, the thickness of the boride layer has an effect on the dimensions and superficial roughness of the materials exposed to the treatment. It has been demonstrated that the dimensions of the borided samples increased by one-fifth to one-third of the total depth of boride layer [3].

In borided low-carbon steels the morphology displayed by both layers is saw-toothed, and the layer-substrate

interface has a columnarity extent as shown in Figure 1(a). Ninham and Hutchings [4] suggested that the columnar nature of the coating interface is caused by dendrite “side arm” growth similar to that seen during the solidification of many metallic systems. In low carbon steels, the boride may “break through” the band of impurities in places, which allows for rapid local boride growth and results in the characteristic saw-toothed interface.

Structural examinations of the surface of high-alloy borided steels reveal the presence of FeB/Fe₂B layers with a flat-front morphology at the growth interfaces (see Figure 1(b) and Figure 1(c)). The development of this morphology can be explained by the high concentrations of alloying elements in the substrate. Alloying elements, such as Cr, Ni, Mo, V and W, are dissolved in the borided layers. However, these alloying elements inhibit the growth of the layers because they are concentrated at the tips of the boride columns via a substitutional procedure. In this way, they decrease the active boron flux in these zones and therefore reduce the columnar shape of the growth in comparison with low-alloying and low-carbon borided steels [5,6]. In addition, they reduce the growth rate of the FeB/Fe₂B layer due to the formation of a diffusion barrier [7], in which a maximum total boride layer thickness of approximately 40-80 μm was formed, depending in the boriding conditions. In the close vicinity of the boronised layers (the diffusion zone), undissolved carbides can be found; these are connected with the carbon diffusion from the borided layer via the bulk material [8].

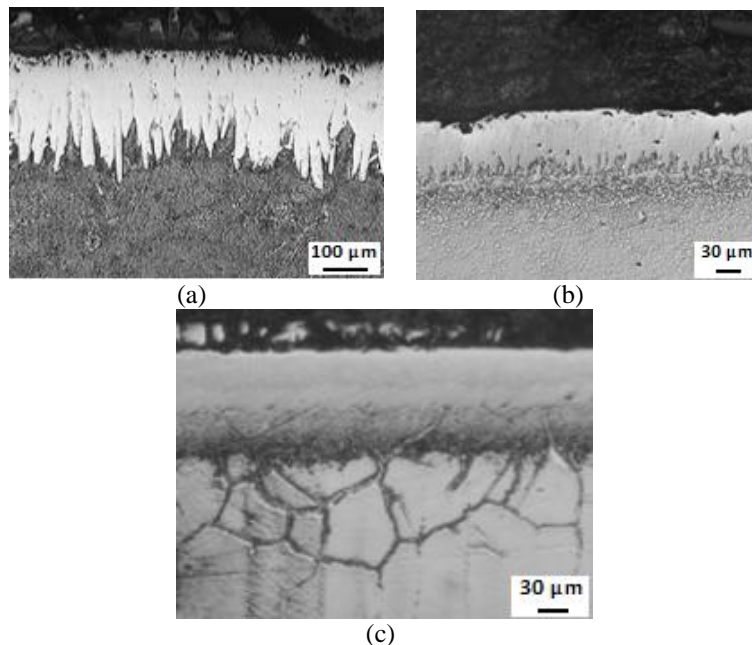


Figure 1 Cross-sectional views of borided samples: (a) AISI 1018 borided steel, (b) AISI M2 borided steel and (c) AISI 316 borided steel. Source: Surface Engineering Group, Instituto Politécnico Nacional, Mexico.

2. The growth kinetics of FeB/Fe₂B layers

Interest in the study of the growth kinetics of boride layers in ferrous alloys has increased over the last twenty years [9-18]. The results of previous studies [1,18,19] have shown that the boride incubation time is dependent on the boriding temperature and decreases with an increase in temperature. Based on the experimental data of the boriding process, which includes exposure time, boride incubation time, temperature, and boron potential of the medium, several kinetic parameters have been estimated, including the weight gain due to the formation of boride layers at the surface of steel, the instantaneous velocity of the Fe₂B/substrate interface, and the boron diffusion coefficients of the FeB/Fe₂B layers, which are dependent on the parabolic growth constant and the (t/t_0) ratio (t is the exposure time of the boriding process, and t_0 is the boride incubation time as a function of the boriding temperature). By the application of Fick's First Law and by properly accounting for material balance at the growing interfaces, simple but comprehensive expressions are obtained for boron diffusion and the growth kinetics of the boride layers.

A linear boron concentration profile was assumed for each of the boride layers formed at the steel surface. C_{up}^i and C_{low}^i represent the maximum and minimum boron concentration in the FeB and Fe₂B layers ($i=$

FeB or Fe₂B), as shown in the Fe-B phase diagram (see Figure 2). The boride layers possessed a narrow range of boron concentrations of about 1 wt.% B. Likewise, the homogeneity of the distribution of boron in the FeB and Fe₂B layers can be described by a₁ and a₃, and the parameters a₂ and a₄ express the miscibility gap between the FeB/Fe₂B and Fe₂B/substrate layers, respectively. Finally, C₀ is the boron concentration in the γ-Fe phase (0.003 wt.% B).

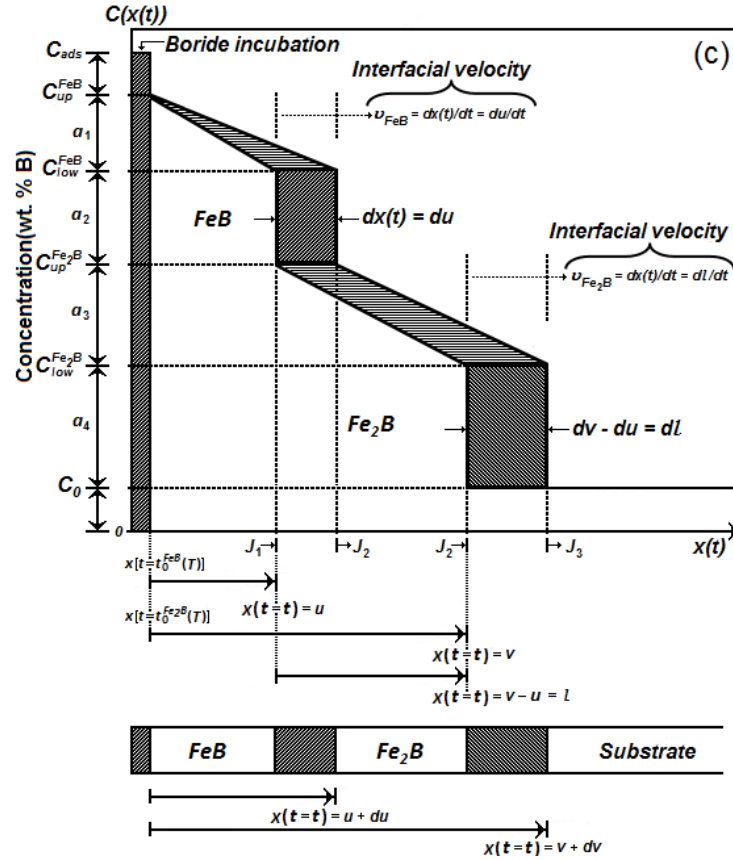


Figure 2 Boron-concentration profile in the FeB and Fe₂B layers [20].

Considering the initial and boundary conditions of the diffusion problem proposed in the Figure 2, the mass balance equations of the FeB/Fe₂B and Fe₂B/substrate interfaces can be described as follows:

$$\Delta_{\text{FeB}} = a_2 du + \frac{1}{2} a_1 du = J_1 dt - J_2 dt \tag{1}$$

$$\Delta_{\text{Fe}_2\text{B}} = a_4 (du + dl) + a_3 du + \frac{1}{2} a_3 dl = J_2 dt - J_3 dt \tag{2}$$

where J_1 , J_2 and J_3 were obtained from Fick's First Law, $J = -D \left\{ \frac{dC[x(t)]}{dx(t)} \right\}$. The equations that represent the boron concentration in the FeB and Fe₂B layers can be described as follows (see Figure 2)

$$C_{\text{FeB}} [x(t)] = C_{\text{up}}^{\text{FeB}} + \frac{C_{\text{low}}^{\text{FeB}} - C_{\text{up}}^{\text{FeB}}}{u} x(t) \tag{3}$$

$$C_{\text{Fe}_2\text{B}} [x(t)] = C_{\text{up}}^{\text{Fe}_2\text{B}} + \frac{C_{\text{low}}^{\text{Fe}_2\text{B}} - C_{\text{up}}^{\text{Fe}_2\text{B}}}{l} [x(t) - u] \tag{4}$$

If the substrate becomes saturated within a short period of time and the solubility of boron is extremely low in γ-Fe (0.003 wt.% B), then $J_3 = 0$. Thus, the fluxes J_1 and J_2 can be expressed by the following equations:

$$J_1 = D_{\text{FeB}} a_1 / u \quad (5)$$

$$J_2 = D_{\text{Fe}_2\text{B}} a_3 / l \quad (6)$$

D_{FeB} is the boron diffusion coefficient of the FeB layer, $D_{\text{Fe}_2\text{B}}$ is the boron diffusion coefficient of the Fe₂B layer, and u and l represent the depth of the FeB and Fe₂B layers, respectively.

The mass balance equations of the interfaces can be expressed as:

$$\frac{du}{dt} = D_{\text{FeB}} P_1 \frac{1}{u} - D_{\text{Fe}_2\text{B}} P_2 \frac{1}{l} \quad (7)$$

$$\frac{dl}{dt} = D_{\text{Fe}_2\text{B}} P_3 \frac{1}{l} - D_{\text{FeB}} P_4 \frac{1}{u} \quad (8)$$

$$\text{with } P_1 = \frac{a_1}{a_2 + a_1 / 2}, \quad P_2 = \frac{a_3}{a_2 + a_1 / 2}, \quad P_3 = a_3 \frac{a_3 + a_4}{a_4 + a_3 / 2} \left(\frac{1}{a_3 + a_4} + \frac{1}{a_2 + a_1 / 2} \right), \quad \text{and}$$

$$P_4 = \frac{a_3 + a_4}{a_4 + a_3 / 2} \left(\frac{a_1}{a_2 + a_1 / 2} \right) \quad (9)$$

The solutions to Eqs. (7) and (8) can be obtained by considering the parabolic growth equations of the surface layers [18-20]:

$$u = k_{\text{FeB}} \left(t - t_0^{\text{FeB}}(T) \right)^{1/2} \quad (10)$$

k_{FeB} is the growth constant of the FeB layer, $t_0^{\text{FeB}}(T)$ is the boride incubation time as a function of the temperature, and $\left(t - t_0^{\text{FeB}}(T) \right)^{1/2}$ is the effective growth time of the FeB layer. In a similar manner, the growth equation of the Fe₂B layer can be defined as:

$$l = v - u = k \left(t - t_0(T) \right)^{1/2} - k_{\text{FeB}} \left(t - t_0^{\text{FeB}}(T) \right)^{1/2} \quad (11)$$

where v is the thickness of the total boride layer, t is the treatment time, $t_0(T)$ is the boride incubation time of the total boride layer ($t_0^{\text{FeB}}(T) > t_0(T)$), and k is the parabolic growth constant of the total boride layer.

Based on the aforementioned assumptions, the boron diffusion coefficients in the FeB and Fe₂B layers ($D_{\text{Fe}_2\text{B}}$ and D_{FeB}) can be expressed by applying Eqs. (7) and (8):

$$D_{\text{Fe}_2\text{B}} = \frac{1}{a_3} \left[(a_4 + a_3 / 2) \left(\frac{du}{dt} + \frac{dl}{dt} \right) + (a_3 / 2) \left(\frac{du}{dt} \right) \right] \quad (\text{m}^2 \text{ s}^{-1}) \quad (12)$$

$$D_{\text{FeB}} = \frac{u}{a_1} \left[(a_4 + a_3 / 2) \left(\frac{du}{dt} + \frac{dl}{dt} \right) + (a_3 / 2 + a_2 + a_1 / 2) \left(\frac{du}{dt} \right) \right] \quad (\text{m}^2 \text{ s}^{-1}) \quad (13)$$

The expressions proposed in Eqs. (12) and (13) can be extended to determine the FeB and Fe₂B layer thicknesses. Furthermore, in the Arrhenius equation, the mean values of the diffusion coefficients are expressed as a function of the temperature, as shown in Figure 3. The activation energy (Q) is obtained from the slope of the graph (Figure 3). The Q value indicates the amount of energy for the boron mobility in the easiest path direction [001] along the boride layer.

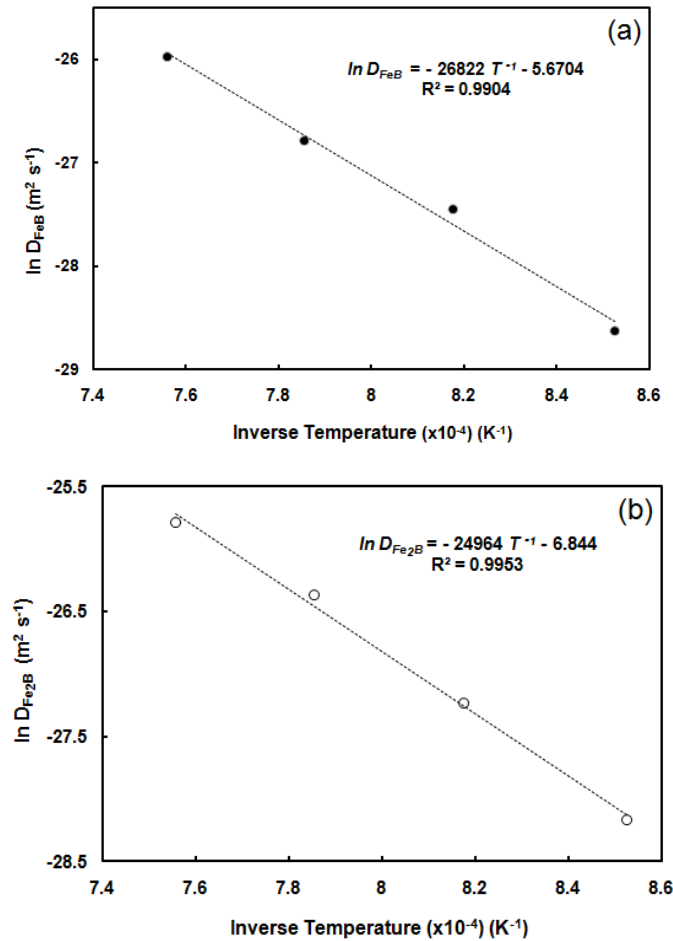


Figure 3. Dependence between the boron diffusion coefficients and boriding temperature: (a) FeB layer, (b) Fe₂B layer. The results are obtained from the boriding of high-alloy steel [20].

3. Mechanical characterization of boride layers

3.1 Fracture-induced Vickers indentation test

One important mechanical parameter in design is the fracture toughness, i.e. K_{IC} . The method of microindentation-induced fracture in brittle materials is a non-destructive and simple technique that requires only a flat and polished surface. Most of the Vickers indentation fracture toughness equations are calibrated using well documented K_{IC} data for a range of brittle materials on the basic assumption that $K_C \equiv K_{IC}$. Hence, the Vickers indentation slow fracture toughness value, in a sense, will be scaled to give the equivalent fast fracture toughness values [21]. The cracks produced by mechanical contact between the indenter and the material surface essentially depend on the geometry of the indenter and the applied load. Radial-median and Palmqvist crack geometry models have been used to determine the fracture toughness in ceramic materials. The theoretical foundation of these models is based on classic concepts of linear elastic fracture mechanics (LEFM) [22].

In recent years, several attempts to determine the fracture toughness (K_C) of different borided steels have been carried out using the Vickers microindentation test. Furthermore, the cracks produced by the indentation load at the corners of the indentation mark were used for this purpose [23-26] as shown in Figure 4. Nevertheless, the motivation for using the radial-median crack regime for the evaluation of K_C in boride layers has not been thoroughly explained. The results of fracture toughness as a function of boriding temperature and exposure time, and varying the indentation loads (0.5 to 10 N), ranged between 2 to 5 MPa \sqrt{m} for the different grades of borided steels.

Furthermore, the fracture toughness of the Fe_2B layers formed at the surface of medium-carbon and low-alloy borided steels was evaluated using the Palmqvist crack regime [19,27]. The fracture toughness was presented as $K_c(\theta)$, where θ is the coordinate angle between the direction of crack propagation and the surface. The results suggest that the fracture toughness decreased with increasing treatment time, and that the K_c values corresponding to the direction of $\pi/2$ were higher ($6 \text{ MPa}\sqrt{\text{m}}$ approximately) than the values obtained in the parallel direction ($3.5 \text{ MPa}\sqrt{\text{m}}$ approximately). This behaviour was a consequence of the high compressive residual stresses that were normal to the surface region and that decreased the crack length in the preferential [001] growth direction of the boride layer.

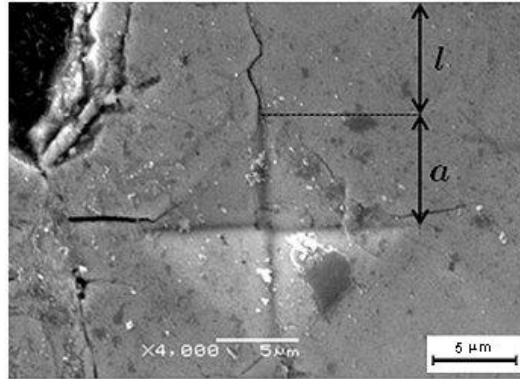


Figure 4. Fracture-induced by Vickers indentation under applied load of 1.96 N on the surface of the Fe_2B layer formed on the AISI 1018 borided steel. a is the half diagonal-length of the indentation mark, l is the crack length. Source: Surface Engineering Group, Instituto Politécnico Nacional, Mexico.

3.2 Berkovich nanohardness test

The methods of micro- and nanoindentation are typically used to investigate the physicochemical properties of boride layers on ultrasmall scales, including the nanometer scale. In recent years, nanoindentation has been developed extensively. This test method is characterized by its simplicity, universality, and the absence of requirements imposed on the specimens and environment. The testing of materials by continuous pressing of the indenter while recording the dependence of the indentation force P on the depth of indentation h (penetration diagram) makes it possible to determine the hardness, elastic modulus, and other physicochemical characteristics of materials, and it is possible to simulate elementary events, such as plastic deformation, fracture, fatigue, cutting, friction, cleavage, creep, elasticity, mass transfer, etc.

A constant indentation load is usually applied along the boride layers to obtain a characteristic hardness-depth profile. The hardness values obtained in the layers are related to the phase composition and the thermal residual stresses produced by the growth of the surface layers, as well as the difference between the specific volume of the substrate and that of the coating [28]. Figure 5 illustrated the Berkovich nanohardness indentations, and the characteristic load-displacement curves obtained on the $\text{FeB}/\text{Fe}_2\text{B}$ layer formed at the surface of borided high-alloy steel.

Furthermore, the behavior of the Young's modulus (E) in both the FeB and Fe_2B layers is related to the morphological and crystallographic anisotropy of the layers, and the influence of the residual stresses acting along the surface [29]. Thus, considering the Young's modulus values in the boride layer obtained by Berkovich nanoindentation, an estimation of the thermal residual stresses (σ_{th}) parallel to the diffusion front can be established from the following expression proposed by Lyakhovich *et al.* [30]:

$$\sigma_{\text{th}} = E_i \left(\frac{\int_{h_i}^{h_2} \alpha \Delta T E_i dh_i}{\int_0^{h_T} E dh_i} - \alpha \Delta T \right) \quad (14)$$

where E is the average of the Young's modulus along the depth of the Fe_2B layer, α is the thermal

expansion coefficient of the Fe_2B layer ($6.9 \times 10^{-6} \text{ } ^\circ C^{-1}$), h_T represents the average thickness of the boride layer, h_i is the thickness of the i -th layer at which the indentation was performed, and ΔT is the interval of cooling temperatures. The Eq. (14) can be extended to estimate the thermal residual stress in both FeB/Fe_2B layers. In addition, Figure 6 shows the behavior of the hardness and the thermal residual stresses in the Fe_2B layer.

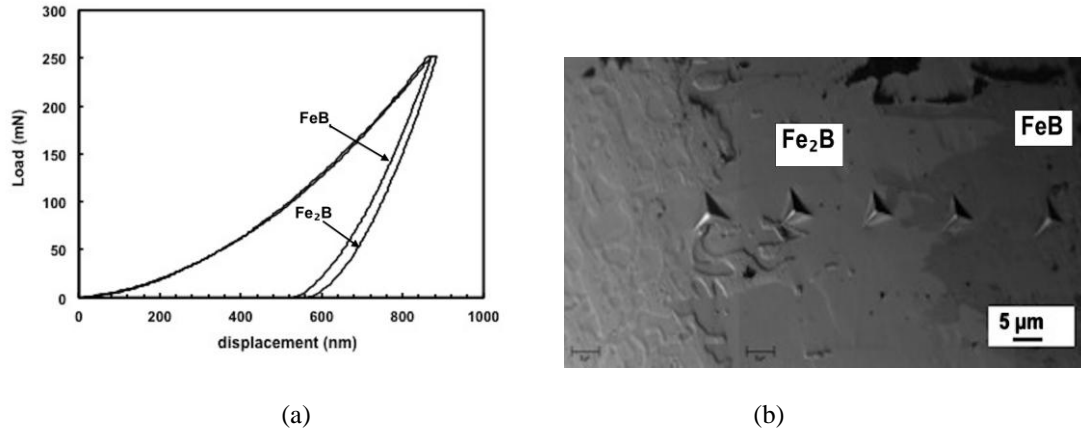


Figure 5. (a) Load-displacement plots obtained in the FeB and Fe_2B layers with an applied load of 250 mN. The boriding temperature was 1273 K with 8 h of exposure, (b) Berkovich indentation marks produced along the boride layers considering the same experimental conditions in (a).

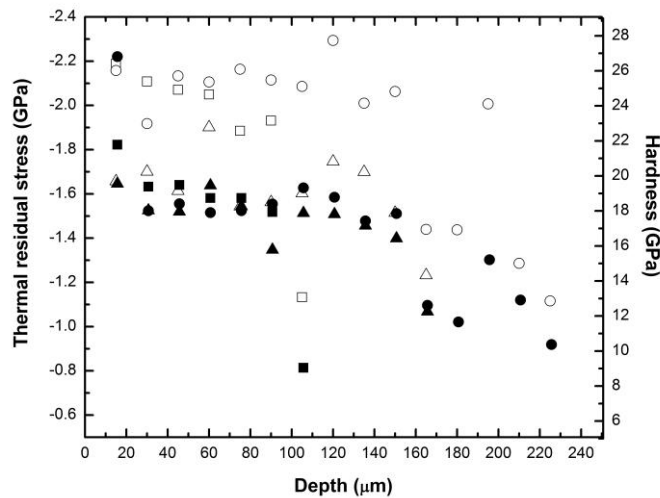


Figure 6. The behavior of hardness and thermal residual stress cross over the boride layer obtained in AISI 1018 steels boriding at a temperature of 1273 K. n hardness at 4 h of exposure, \blacktriangle hardness at 6 h of exposure, γ hardness at 8 h of exposure, \square thermal residual stress at 4 h of exposure, Δ thermal residual stress at 6 h of exposure, and ϕ thermal residual stress at 8 h of exposure. Source: Surface Engineering Group, Instituto Politécnico Nacional, Mexico.

The surface hardness obtained by the boriding process depended mainly on the temperature, exposure time, alloying elements of the substrate (in this case, the carbon has very little influence on the hardness of the boride layer), the boron potential at the surface of the steel, and the formation of layers of one or two phases [20]. Because of the high hardness gradient between the Fe_2B layer and the steel substrate, which causes the brittleness of the coated system, the high hardness achieved in steel exposed to boriding is not always recommended or beneficial. One advantage of the boriding process is that the boride layer maintains its hardness up to 1173 K, which allows the use of a wide range of temperatures for post-heat treatments. The thermal residual stresses estimated from Eq. (14) (considering the behavior of the Young's modulus obtained in the nanoindentation testing on the Fe_2B layer) established a compressive state with higher values near the surface region. The nature of the compressive thermal residual stresses in the Fe_2B layer can be

explained by the fact that the substrate shrinks more than the boride layer upon cooling because of its larger coefficient of linear expansion. Consequently, a thermally induced compressive strain must be imposed on the layer to attach the layer to the substrate at temperatures below the boriding temperature. Also, the presence of compressive stresses in the boride layer is beneficial because they increase the capacity for static tensile loads.

4. Conclusions

This study proposed a diffusion model to estimate the boron diffusion coefficients of the FeB/Fe₂B layer formed at the surface of different grades of borided steels. The diffusion model was based on the boron concentration profiles of the surface layers, the parabolic growth law, which considers the boride incubation time, and the mass balance equations of the FeB/Fe₂B and Fe₂B/substrate interfaces. The model can be extended to evaluate variations in the thickness of the FeB/Fe₂B layer, for a particular industrial application. In addition, based on the Vickers and nanohardness techniques, some mechanical properties of the boride layers can be estimated; the fracture-induced Vickers indentation method is an alternative for characterizing the adhesion properties of hard coatings, and in fact, the wear resistance of the boride layers. In addition, for the nanoindentation technique, the behavior of the hardness values can be established according to the state of the compressive thermal residual stresses in the boride layer, which can be determined by the distribution of the Young's modulus across the layer. Compressive residual stresses are known to improve the service behavior of borided steels.

Acknowledgements

This work was supported by the research grants 150556 of the CONACyT and 20120594 of the *Instituto Politécnico Nacional* of Mexico. The authors wish to thank the Nanosciences Center and Micro-Nano Technologies of the Instituto Politécnico Nacional for their cooperation

References

1. Campos-Silva I., Ortiz-Dominguez M., Cimenoglu H., Escobar-Galindo R., Keddani M., Elías-Espinosa M. and Lopez-Perrusquia N., Diffusion model for growth of Fe₂B layer in pure iron, *Surf. Eng.* Vol. 27, 189-195, 2011.
2. Davis J.R., *Surface Hardening of Steels: Understanding the Basics*. ASM International, Ohio, 2002
3. Sahin S., Effects of boronizing process on the surface roughness and dimensions of AISI 1020, AISI 1040 and AISI 2714, *J. Mater. Process. Technol.* Vol. 209, 1736-1741, 2009.
4. Ninham, A.J. and Hutchings, I.M., On the morphology of thermochemically produced Fe₂B/Fe interfaces, *J. Vac. Sci. Technol.* Vol. A 4, 2827-2831, 1986.
5. Goeriot, P., Fillit, R., Thevenot, F., Driver, J. H. and Bruyas, H., The influence of alloying element additions on the boriding of steels, *Mater. Sci. Eng.* Vol 55, 9-19, 1982.
6. Carbucchio, M. and Palombarini, G., Growth of boride coatings on iron, *J. Mater. Sci. Lett.* Vol. 6, 1147-1149, 1987.
7. Matiasovsky, K., Chrenkova-Paucirova, M., Fellner, P. and Makyta, M., Electrochemical and thermochemical boriding in molten salts, *Surf. Coat. Technol.* Vol. 35, 133-149, 1988.
8. Jurci, P. and Hudakova, M., Diffusion boronizing of H11 hot work tool steel, *J. Mater. Eng. Perform.* doi: 10.1007/s11665-010-9750-x, 2011.
9. Brakman, C.M., Gommers, A.W.J. and Mittemeijer, E.J., Boriding of Fe and Fe C, Fe-Cr, and Fe-Ni alloys: Boride layer growth kinetics, *J. Mater. Res.* Vol.4, 1354-1370, 1989.
10. Pelleg, J. and Judelewicz, M., Diffusion in the B-Fe system and compound formation between electron gun deposited boron thin films and steel substrate, *Thin Solid Films* Vol. 215, 35-41, 1992.
11. Raic, K., Acimovic, Z., Vidojevic, N. and Novovic-Simovic, N., Modelling of Fe₂B boride layer growth, *J. Serb. Chem. Soc.* Vol. 61, 181-188, 1996.
12. Meléndez, E., Campos, I., Rocha, E. and Barrón, M.A., Structural and strength characterization of steels subjected to boriding thermochemical process, *Mater. Sci. Eng. A*, Vols. 234-236, 900-903, 1997.
13. Campos I., Oseguera, J., Figueroa, U., García, J.A., Bautista, O. and Kelemenis, G., Kinetic study of boron diffusion in the paste boriding process, *Mater. Sci. Eng. A*. Vol. 352, 261-265, 2003.
14. Sen, S., Sen, U. and Bindal, C., An approach of kinetic study of borided steels, *Surf. Coat. Technol.* Vol. 191, 274-285, 2005.
15. Yu, L.G., Chen, X.J., Khor, K.A. and Sundararajan, G., FeB/Fe₂B phase transformation during SPS pack-boriding: Boride layer growth kinetics, *Acta Mater.* Vol. 53, 2361-2368, 2005.

16. Keddad M., Computer simulation of monolayer growth kinetics of Fe₂B phase during the paste-boriding process: Influence of the paste thickness, *Appl. Surf. Sci.* Vol. 253, 757-761, 2006.
17. Dybkov, V.I., Growth of boride layers on the 13% Cr steel surface in a mixture of amorphous boron and KBF₄, *J. Mater. Sci.* Vol. 42, 6614-6627, 2007.
18. Campos-Silva I., Ortiz-Domínguez, M., Keddad, M., López-Perrusquia, N., Carmona-Vargas, A. and Elias-Espinosa, M., Kinetics of the formation of Fe₂B layers in gray cast iron: Effects of boron concentration and boride incubation time, *Appl. Surf. Sci.* Vol. 255, 9290-9295, 2009.
19. Campos-Silva, I., Ortiz-Domínguez, M., López-Perrusquia, N., Meneses-Amador, A., Escobar-Galindo, R. and Martínez-Trinidad, J., Characterization of AISI 4140 borided steels, *Appl. Surf. Sci.* Vol. 256, 2372-2379, 2010.
20. Campos-Silva, I., Ortiz-Domínguez, M., Tapia-Quintero, C., Rodríguez-Castro, G., Jiménez-Reyes, M.Y. and Chávez-Gutiérrez, E., Kinetics and boron diffusion in the FeB/Fe₂B layers formed at the surface of borided high-alloy steel, *J. Mater. Eng. Perform.* doi: 10.1007/s11665-011-0088-9, 2011.
21. Ponton, C.B. and Rawlings, R.D., Vickers indentation fracture toughness test Part 1 Review of literature and formulation of standardized indentation toughness equations, *Mater. Sci. Technol.* Vol. 5, 865-872, 1989.
22. Ponton, C.B. and Rawlings, R.D., Vickers indentation fracture toughness test Part 2 Application and critical evaluation of standardized indentation toughness equations, *Mater. Sci. Technol.* Vol. 5, 961-976, 1989.
23. Bindal, C. and Ucisk, A., Characterization of borides formed on impurity-controlled chromium-based low alloy steels, *Surf. Coat. Technol.* Vol. 122, 208-213, 1999.
24. Ozbek, I. and Bindal, C., Mechanical properties of boronized AISI W4 steel, *Surf. Coat. Technol.* Vol. 154, 14-20, 2002.
25. Uslu, I., Comert, H., Ipek, M., Celebi, F. G., Ozdemir, O. and Bindal, C., A comparison of borides formed on AISI 1040 and AISI P20 steels, *Mater. and Des.* Vol. 28, 1819-1826, 2007.
26. Celebi, F. G., Ipek, M., Ozbek, I. and Bindal, C., Kinetics of borided 31CrMoV9 and 34CrAlNi7 steels, *Mater. Charac.* Vol. 59, 23-31, 2008.
27. Campos, I., Rosas, R., Figueroa, U., VillaVelázquez, C., Meneses, A. and Guevara, A., Fracture toughness evaluation using Palmqvist crack models on AISI 1045 borided steels, *Mater. Sci. Eng. A.* Vol. 488, 562-568, 2008.
28. Galibois A., Boutenko, O. and Voyzelle, B., Mécanisme de formation des couches borurées sur les aciers a haut carbone – I. *Technique des pates*, *Acta Metall.* Vol. 28, 1753-1763, 1980.
29. Byakova, A. V., Influence of texture on the strength and supporting capacity of boride coatings, *Poroshkovaya Metallurgiya* Vol. 4, 36-43, 1993.
30. Lyakhovich, L. S., Kosachevskii, L. N., Kulik, Ya. A., Surkov, V. V. and Turov, Yu. V., Possibility of predetermining the distribution of residual stresses in borided steels, *Fiziko-Khimicheskaya Mekhanika Materialov* Vol. 9, 34-37, 1973.